Malaysian Journal of Chemistry, 2026, Vol. 28(1), 31-40
(Special Issue: *3rd International Conference on Industry-Academia Initiatives in Biotechnology & Chemistry, iCIABC2025*)

Dual-Response Hexagonal Boron Nitride in Epoxy Vitrimer Nanocomposite for Self-Repairable and Corrosion Resistance Coatings

Nurul Fatihah Norapandi[1], Aiman Sofiah Razlan[1], Kwok Feng Chong[1,2], Nurjannah Salim[1,2], Siti Maznah Kabeb[1,2], Rasidi Roslan[1,2] and Nurul Huda Abu Bakar[1,2]*
[1]Faculty of Industrial Sciences & Technology, Universiti Malaysia Pahang Al-Sultan Abdullah, Gambang Campus, 26300, Kuantan Pahang, Malaysia
[2]Centre for Advanced Intelligent Materials, Universiti Malaysia Pahang Al-Sultan Abdullah, Gambang Campus, 26300, Kuantan Pahang, Malaysia
*Corresponding author (e-mail: hudabakar@umpsa.edu.my)

Epoxy vitrimers (EV) are known for their self-repairing properties, utilizing dynamic disulfide bonds that reformed under heat. However, their brittleness and softness limit practical use. Hexagonal boron nitride (hBN), with its high thermal conductivity and mechanical reinforcement, offers a solution. This study explores hBN at 0.5 wt.% and 1.0 wt.% in EV to assess self-repairing, mechanical integrity, and corrosion resistance. The 0.5 wt.% hBN formulation achieved rapid self-repairing in ~10 minutes, demonstrating hBN's role in efficient heat transfer and bond reformation. The 1.0 wt.% formulation showed superior corrosion resistance and hydrophobicity due to hBN's barrier properties. Knife-scratch tests revealed severe delamination in pure epoxy vitrimer, moderate in 1.0 wt.% hBN, and a clean cut in 0.5 wt.% hBN, indicating better mechanical integrity. Both loadings highlight hBN's dual role in enhancing self-repairing and mechanical integrity. The study underscores the critical role of hBN dosage, as excess loading can compromise performance, offering insights for designing advanced self-repairing coatings.

Keywords: Copper, self-healing, wettability, disulfide bonds, 2D materials

Received: June 2025; Accepted: November 2025

Epoxy coatings are widely recognized as one of the most effective protective barriers for metallic substrates due to their excellent adhesion, mechanical strength, and chemical resistance. When applied to steel or copper surfaces, these coatings form a dense, cross-linked polymeric network that limits the permeation of corrosive species such as water, oxygen, and chloride ions [1, 2]. However, the intrinsic brittleness and microdefect formation in conventional epoxy coatings can eventually lead to coating degradation and localized corrosion [3]. To overcome these challenges, epoxy systems are often modified or added with functional fillers or reactive components to enhance their barrier integrity and long-term corrosion protection performance.

In recent years, there has been increasing interest in developing epoxy with self-healing ability via intrinsic or extrinsic mechanisms [4-7]. Extrinsic self-healing refers to the coating's ability to autonomously recover its properties and restore functionality after damage, without requiring external physical intervention. It can be synthesized by embedding microcapsules containing the healing agents into the coating matrix [8]. However, the microcapsule shell must be rigid enough to maintain structural integrity during the service life, yet sufficiently fragile to rupture reliably upon mechanical damage and release the healing agent. This dual requirement presents a fundamental challenge in designing the system for optimal performance [9]. In contrast, intrinsic self-healing (or self-repairable) coatings require external activation, such as heat, and are classified as non-autonomous. The reformation of bonds effectively seals microscopic cracks, preventing the propagation of damage and mitigating the initiation of corrosion. In addition, self-repairable coatings are highly versatile and can be applied across various industries, such as aerospace, marine, automotive, and infrastructure, where controlled activation is essential.

In polymer technology, a novel class of polymers known as "vitrimers" was introduced by Ludwik Leibler [10]. Vitrimers exhibit dynamic covalent bonding, enabling them to merge the reprocessability of thermoplastics with the mechanical stability and durability of thermosets. Notably, the dynamic disulfide bonds in 2-aminophenyl disulfide (APD) incorporated into epoxy systems have been extensively studied for their self-repairable properties, including enhanced chemical stability and corrosion resistance [11].

†Paper presented at the 3rd International Conference on Industry-Academia Initiatives in Biotechnology & Chemistry

Furthermore, nanocomposite epoxy vitrimer (EV) systems, such as those fabricated with graphene oxide, have demonstrated exceptional self-repairing capabilities [5]. Additionally, the vitrimer coating of APD/epoxy has been effectively utilized as a protective coating for carbon steel. The protective performance is attributed to the disulfide bond exchange mechanism, which occurs without any chemical degradation or alterations [12]. However, the vitrimer's inhibitory capability may be limited to some degree by its porous structure.

An effective strategy to enhance the porous structure of EV, is the incorporation of inorganic 2D materials like hexagonal boron nitride (hBN). hBN consists of B and N atoms arranged in hexagonally planar rings that are bonded by a strong sp^2 covalent bond [13]. Their layered structures are held by van der Waals forces. It has excellent physical properties, including a high Young's modulus, hardness, eco-friendliness, and good chemical stability [14]. Research on nanocomposites comprising hBN and various polymers is on the rise due to its promising properties. For example, studies on polyaniline, polystyrene, and copolymers of vinyl chloride-acrylonitrile have demonstrated that the inclusion of hBN significantly enhances the mechanical properties of coatings, offering superior durability and functionality [15].

Hence, the present study focuses on the self-repairable and corrosion-resistant properties of EV-*x*hBN nanocomposite coatings. A comprehensive evaluation of the vitrimeric epoxy nanocomposite coatings was performed by varying the hBN dose in the EV matrix, specifically at x = 0.5 and 1.0 wt.%, where x is denoted as hBN weight percentage. Additionally, the wettability of the prepared nanocomposite coatings was analyzed to establish a correlation with their corrosion inhibition performance in a 3.5% NaCl electrolyte simulation. The interaction between hBN and the EV matrix was further confirmed through Fourier Transform Infrared Spectroscopy (FTIR), providing deeper insights into the material's structural and chemical compatibility. The morphological characteristics of the coatings after knife-scratching and self-repair by thermal stimuli were observed using metallurgical microscopy and Scanning Electron Microscopy (SEM) for better evaluation.

EXPERIMENTAL

Chemicals and Materials

The diglycidyl ether of bisphenol A (DGEBA) epoxy resin (BE-188) was purchased from Mc-Growth Chem. 2-aminophenyl disulfide (APD) used as a hardener, hexagonal Boron Nitride (<150, 99%), and Ethanol-95% (C_2H_5OH) were purchased from Sigma-Aldrich. Dimethylformamide (DMF) was purchased from Kollin Chemicals. The Cu substrates were supplied by Shandong Shengxin Technology Co. Ltd.

EV and EV-*x*hBN Preparation

Approximately 500 mg of APD was dissolved in 0.25 mL DMF under ultrasonication for 1 h. The mixture was then added to epoxy resin and stirred vigorously. The mixture was labeled as EV. The Cu substrates were polished sequentially with 80, 500, and 100 grit sandpaper and ultrasonically cleaned with deionized water and acetone. The EV was coated onto 2 × 2 cm Cu substrates using the drop coating method for thermal-responsive self-repair. On the other hand, the EV mixture was drop-coated onto 5 × 1 cm Cu substrates for corrosion performance evaluation. The coated samples were cured at 80 °C until the solvent completely evaporated.

Meanwhile, EV-*x*hBN nanocomposite coatings were prepared by adding two different hBN loading i.e., 0.5 wt.% and 1.0 wt.%. The specific preparation steps are as follows, taking 0.5 wt.% as an example. First, 5 mg of hBN was ultrasonically dispersed in 1 mL of ethanol for 30 minutes and was added to 1 mL of epoxy resin. Next, the APD/DMF mixture was added to the epoxy resin and stirred. Then, the nanocomposite coating was coated on Cu steel with the same method as in the previous one. For better insight into the performance, the pure EV coating and EV-*x*hBN nanocomposite coatings were compared for wettability, thermal responsiveness, and electrochemical analysis.

Characterization Methods

The chemical properties of the prepared EV and EV-*x*hBN nanocomposite were studied using Fourier transforms infrared spectroscopy (FTIR) by Perkin Elmer (Model Spectrum 100). The FTIR was conducted using the Potassium Bromide Disk (KBr) method with spectral range from 4000 to 400 cm^{-1} at a resolution of 4 cm^{-1} at ambient temperature. The wettability properties of the coatings were evaluated using water contact angle, measured with a static contact angle analyzer (OCA 15EC) at a volume of 5 µL. The thickness of the prepared coatings was measured using micrometer screw gauge at five different flat spots on the coatings' surfaces and average values were calculated. The coating thickness was obtained by subtracting the uncoated substrate thickness from the coated substrate thickness. All substrate areas were maintained for each coating to ensure accuracy.

The adhesion of the coatings was evaluated using a knife adhesion test in accordance with ASTM D6677. The mechanical indentation of the samples was evaluated using Vickers hardness tester (Wilson

Instruments 402 MVD) with a 200gf load and a dwell time of 10 seconds. Each sample had three measurements taken, and the average was selected. The hardness number (HV) was calculated using Equation (1).

$$HV = 1854.4 \times \frac{F}{d^2} \quad \text{Eq. (1)}$$

where F is the applied force and d is the average diagonal length. To evaluate self-repairing ability, the nanocomposite coatings were knife-scratched and heated to 60 °C for 10 minutes in a universal oven. The images of the samples were captured using a metallurgical microscope (Olympus BX51RF) at 100X magnification before and after heat exposure. The changes of scratch width were analyzed by ImageJ software and the self-repairing efficiency was calculated using Equation (2). Each sample had three measurements taken, and the average was selected.

$$\text{Self-repairing efficiency} = \frac{width\ before\ sctrath\ (\mu m) - width\ after\ \ sctrath(\mu m)}{width\ before\ sctrath\ (\mu m)} \times 100\% \quad \text{Eq. (2)}$$

The detail analysis on the nanocomposite coatings surface morphology was conducted using Scanning Electron Microscope (SEM: FEI Quanta 450, EDX: Oxford). Further corrosion performance of the samples was evaluated using potentiodynamic polarization (Tafel plots) with a three-electrode system. The coated sample is the working electrode (WE), platinum wire as the counter electrode (CE), and silver chloride (Ag/Cl) as the reference electrode (RE). The corrosion test was conducted in a 3.5 % NaCl electrolyte to imitate the common corrosive media. The frequency range used was from 10 mHz to 100 kHz with a 10 mV amplitude voltage using Autolab M101. The corrosion rate (CR) was calculated from the corrosion current values using Equation (1) [16];

$$CR\left(\frac{mm}{yr}\right) = \frac{\left(I_{corr} \times K \times EW\right)}{\rho A} \quad \text{Eq. (3)}$$

RESULTS AND DISCUSSION

Chemical Properties and Elemental Composition

The chemical functional groups of the precursor materials comprising hBN, pure epoxy, EV, and EV-1hBN nanocomposites were characterized using FTIR, as shown in Figure 1. All samples exhibited broad absorption peaks between 3300 and 3500 cm^{-1}, corresponding to OH stretching vibrations. In the EV and EV-1hBN samples, these bands appeared more complex due to overlapping OH stretching from the amine hardener (APD), indicating th e presence of hydrogen bonding within the vitrimer network. The absorption peaks between 2800 and 3100 cm^{-1} are assigned to aromatic and aliphatic C–H stretching vibrations, mainly contributed by APD and the epoxy backbone. A distinct band around 1700 cm^{-1}, present in all samples except hBN, corresponds to the C=O stretching of the epoxy matrix. Peaks around 1300 cm^{-1} arise from ether linkages (COC) in the epoxy resin, which overlap with CN stretching from APD and BN vibrations from hBN [17]. Importantly, in the EV-1hBN spectrum, the characteristic B–N stretching peak of hBN near 1370 cm^{-1} and the B–N–B bending band at 800 to 900 cm^{-1} remain visible without any significant shift or intensity loss. This observation indicates that the B–N structure of hBN remains chemically unaltered after incorporation into the vitrimer matrix. Likewise, the absorption band between 500 and 700 cm^{-1}, attributed to S–S bonds from the disulfide-containing APD, remains distinct in both EV and EV-1hBN. The coexistence of unshifted B–N and S–S bands confirms that hBN does not chemically react with or disrupt the disulfide linkages.

These FTIR findings support the conclusion that hBN acts as an inert filler within the vitrimer system, interacting physically rather than chemically with the polymer network. As a result, the intrinsic disulfide exchange and surface wettability properties of the epoxy vitrimer are preserved, consistent with the stable interfacial compatibility and nonreactive nature of hBN.

The morphology and elemental composition of the hBN precursor were analyzed by SEM-EDX to confirm the presence of B and N, as shown in Figure 2. The hBN exhibited a sheet-like conglomerate and disc-like morphology with a diameter of 190 – 300 nm, consistent with previous studies [18, 19]. The size of the particles confirmed its nanostructure properties, making it suitable for epoxy filler use. The elemental composition of hBN were verified through EDX analysis, achieving a 0.8:1 ratio of B to N, matching the expected stoichiometry. The results of the EDX analysis confirmed the purity of the hBN precursor.

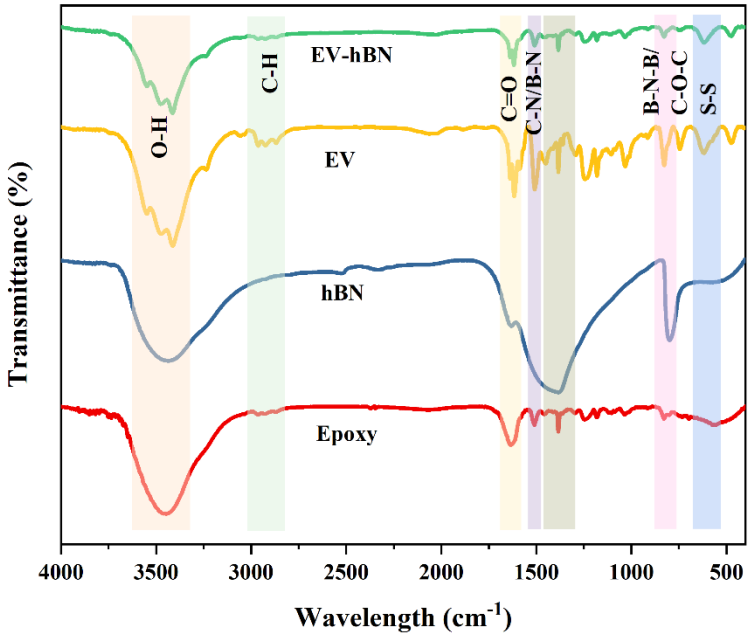

Figure 1. FTIR spectra of hBN, Epoxy, EV and EV-hBN nanocomposite.

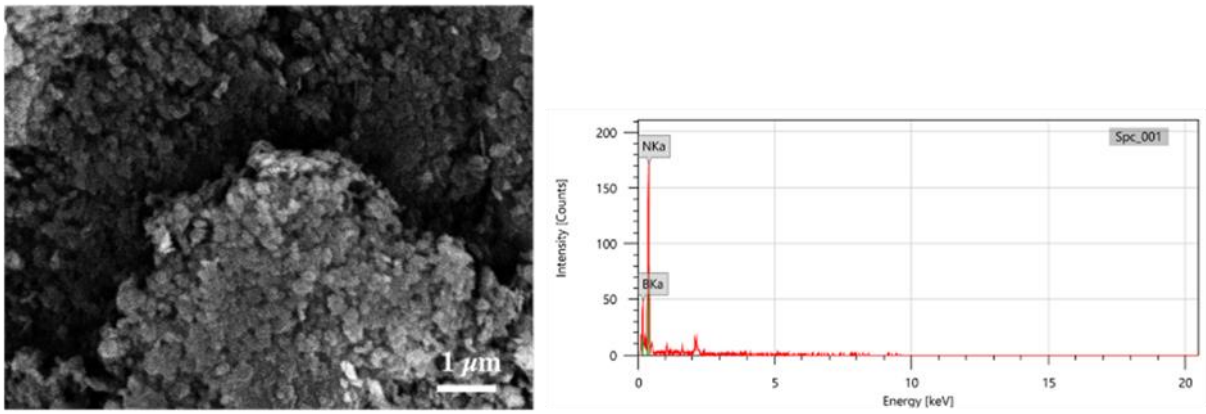

Figure 2. Morphology and elemental composition of hBN.

Performance of EV-*x*hBN Nanocomposite Coatings

Thickness and Mechanical Integrity

The thickness, adhesion and indentation depth of the EV and EV-*x*hBN nanocomposite coatings were evaluated to comprehend the coatings' integrity. Due to the epoxy's viscosity and addition of hBN nanoparticles, the thickness of all coatings was observed to be in the range of 650 µm to 700 µm. For the adhesion test, no delamination was observed after the tape was removed, indicating good adhesion between the coatings and the substrate as shown in Figure 3(a). However, the extent of cutting damage varied among the samples. The pure EV coating exhibited severe cutting, suggesting poor resistance to mechanical stress. The 1.0 wt.% hBN formulation showed moderate damage, while the 0.5 wt.% hBN formulation demonstrated the least cutting damage, with a clean and well-defined cut. This indicates that adding hBN, particularly at 0.5 wt.%, significantly improves the coating's mechanical integrity and resistance to damage, likely due to enhanced dispersion and reinforcement effects at lower loadings.

The mechanical indentation of the coatings on copper substrates shows varying penetration depth and width Figure 3(b). As summarized in Table 1. EV has lower mechanical strength due to its viscous solution, resulting in a soft and brittle coating with a hardness number (HV) of 20.7 and penetration depth of 7.6 µm.

The sample EV-0.5hBN formulation exhibits a higher HV of 23.9 with a corresponding penetration depth of 4.6 µm. EV-1hBN had a less viscous solution, yielding an HV value of 21.7 and a penetration depth of 6.0 µm. The penetration depth for all samples is lower than the coating thickness, indicating low impact of the substrates on the mechanical performance. It is worth mentioning that EV had a trace of cracking near the indentation mark, suggesting brittleness. Although EV-*x*hBN samples have a larger indentation width but there is no sign of cracking, suggesting flexibility and resistance to mechanical stress.

Wettability Properties

The water contact angle (WCA) results are shown in Figure 4 with the average WCA of EV is 94.4°, EV-0.5hBN is 99.8° and EV-1hBN is 103.2°. All coatings exhibit hydrophobic properties, with a notable 8.5% increase in hydrophobicity observed at an hBN concentration of 1.0 wt.%. Notably, the relationship between hBN content and water contact angle (WCA) highlights that as hBN concentration increases, the hydrophobicity of the nanocomposite material is significantly enhanced. This is due to the increased surface area of hBN particles, which disrupts the continuity of polar interactions within the polymer matrix, thereby promoting a more hydrophobic surface. The phenomenon decreases surface wettability by creating a more water-repellent surface due to its inherent low surface energy and nano-scale roughness [20]. It is also suggested that hBN does not chemically interact with the disulfide bonds due to its inert nature, thereby the wettability properties still preserve [21]. As a result, the EV-*x*hBN coating becomes more resistant to water penetration, making it highly suitable for applications requiring superior water-repellent properties.

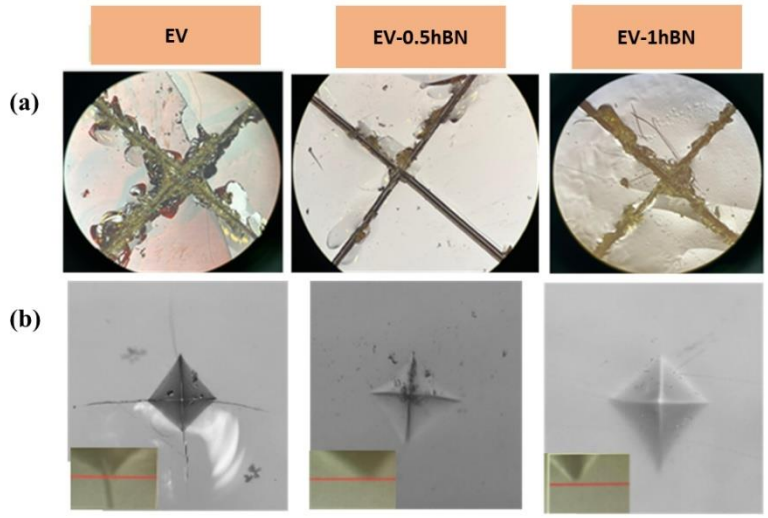

Figure 3. (a) Knife-scratch and (b) indentation test for EV EV-0.5hBN and EV-1hBN.

Table 1. Mechanical indentation data for epoxy nanocomposite coatings.

Sample (wt.%)	Hardness number (HV)	Penetration depth (µm)
EV	20.7	7.6
EV-0.5hBN	23.9	4.6
EV-1hBN	21.7	6.0

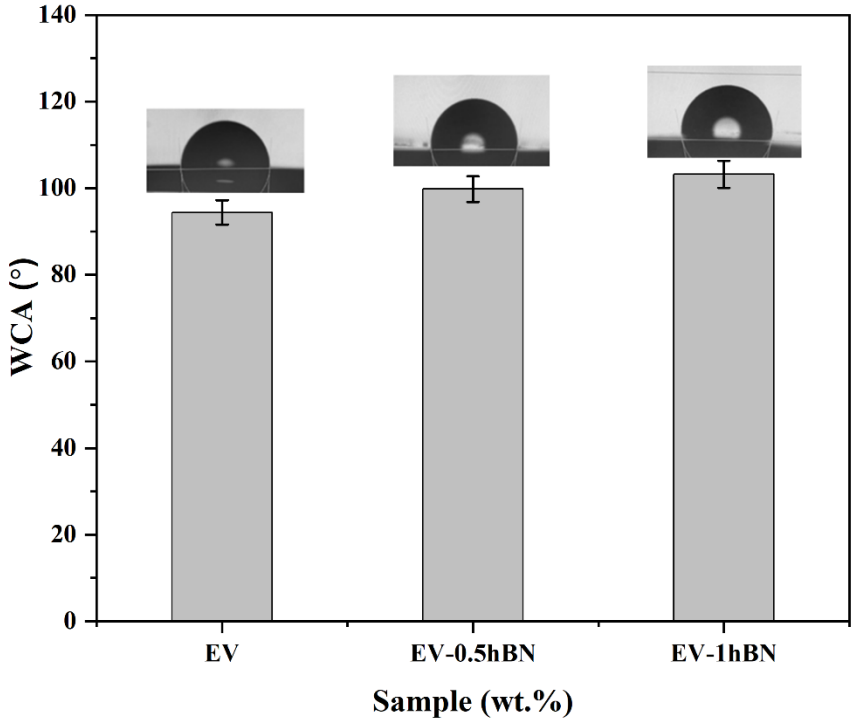

Figure 4. WCA of EV and EV-*x*hBN coatings.

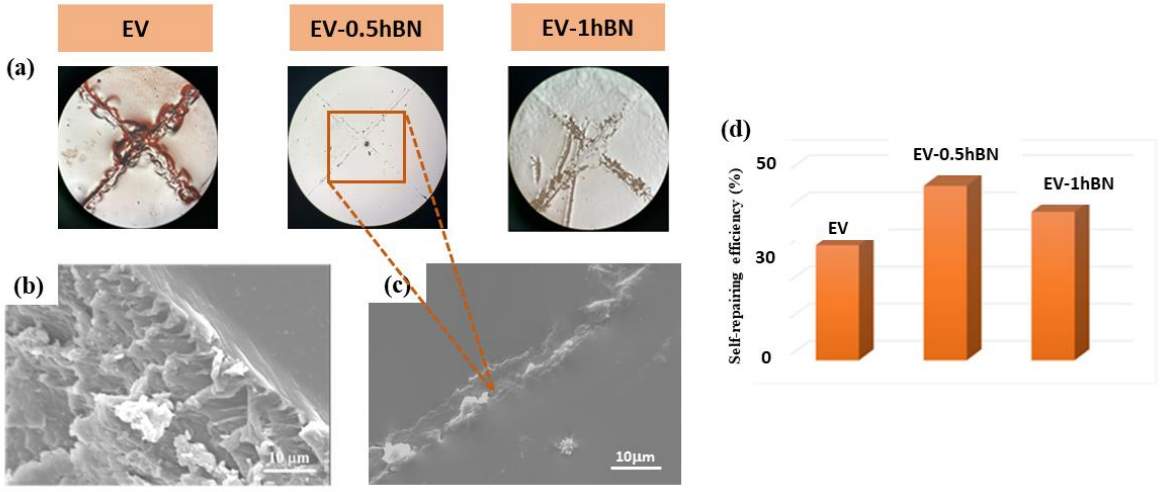

Figure 5. (a) Healed knife-scratched of EV and EV-*x*hBN at 60 °C for 10 minutes, (b & c) morphology of 0.5% hBN before and after self-repair and (d) efficiency (%).

Self-repairing Characteristics

The self-repairing performance of EV and EV-*x*hBN nanocomposites coatings was evaluated by observing the knife-scratched damage and was recorded in Figure 5 (a). All the samples exhibit self-repairable behavior after the heat exposure due to disulfide-mediated radical exchanges and S–S bond rearrangement [12, 22]. For nanocomposite sample, EV-0.5hBN recorded the highest self-repair efficiency (~68%) as compared to EV-1hBN (~40%). The addition of hBN improves the time taken for damage repair due to its high thermal conductivity. According to previous research [24], this property enhances the heat flow across the epoxy vitrimer matrix, hence improving the self-repair ability. Nevertheless, higher hBN loadings limit the repairing process. This might be attributed to excess hBN creating a dense network that restricts the chain mobility in epoxy vitrimer network, affecting the

dynamic bond exchange. Joy et al. [24] verified that the incorporation of hBN filler in the polymer chain increases the glass transition temperature (T_g), which is associated with the molecular motion. Further morphological characterization of the EV-0.5hBN nanocomposite coating was conducted using SEM, as presented in Figure 5 (b) and (c). Prior to thermal treatment, the scratched region exhibits a linear fracture morphology accompanied by flaky pieces (Figure 5b). Following exposure to thermal stimuli, the same area displayed a markedly smoother surface with visible closure of the scratch (Figure 5c), conforming to active self-repair.

Corrosion Resistance

Figure 6 demonstrated the potentiodynamic polarization curves (Tafel plots) of EV and EV-*x*hBN nanocomposites coatings on copper substrates. The anodic slopes (β_a), cathodic slopes (β_c), corrosion potential (E_{corr}), corrosion current (I_{corr}), corrosion rate (CR), and resistance potential (R_p) are summarized in Table 2. It can be observed that β_a and β_c become flatter with the addition of hBN, indicating hBN reduces the kinetics of both anodic and cathodic reactions, contributing to the improved corrosion resistance of copper substrates. Besides, E_{corr} values of the samples coated EV, EV-0.5hBN and EV-1hBN shifted towards a positive value from -0.188 to -0.168 and -0.079 V, respectively. This shifting confirmed the good barrier protection of hBN epoxy vitrimer nanocomposite [25]. In addition, compared to EV, I_{corr} values of the samples coated EV-0.5hBN and EV-1hBN decreases from 1.217 µA/cm^2 to 1.029 and 0.384 µA/cm^2, which further verifies the inhibition action of the composite.

Meanwhile, a lower CR was recorded with the increasing hBN content. 2D hBN filler plays a crucial role in prolonging the penetration path of corrosive iron towards the underlying metal, which can be called the "labyrinth effect" phenomenon [26]. The modification with hBN nanofiller might blocked the flaws formed in the epoxy vitrimer coating, resulting in the development of a compact structure. Moreover, the hydrophobic character of EV-*x*hBN coating repelled the NaCl electrolyte, resulting in diffusion away from the steel substrate [27]. R_p values were found to be increased with the increase of hBN content. It represents the copper's resistance to oxidation when subjected to an external potential, where their values were inversely proportional to the I_{corr}.

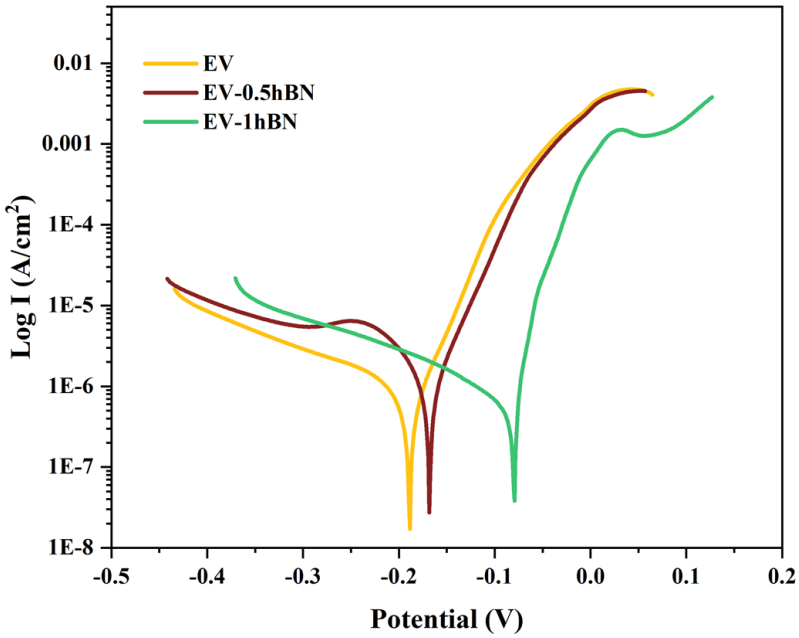

Figure 6. Tafel plots of EV and EV-*x*hBN.

Table 2. Corrosion parameter of APD/Epoxy and APD-*x*hBN/Epoxy

Sample	E_{corr} (V)	I_{corr} (µA/cm^2)	β_a (mV/dec)	β_c (mV/dec)	CR (mm/year)	R_p (Ω cm^2)
EV	-0.188	1.217	25.34	64.38	0.014	6.49
EV-0.5hBN	-0.168	1.029	61.59	42.74	0.012	10.65
EV-1hBN	-0.079	0.384	79.76	11.38	0.004	11.26

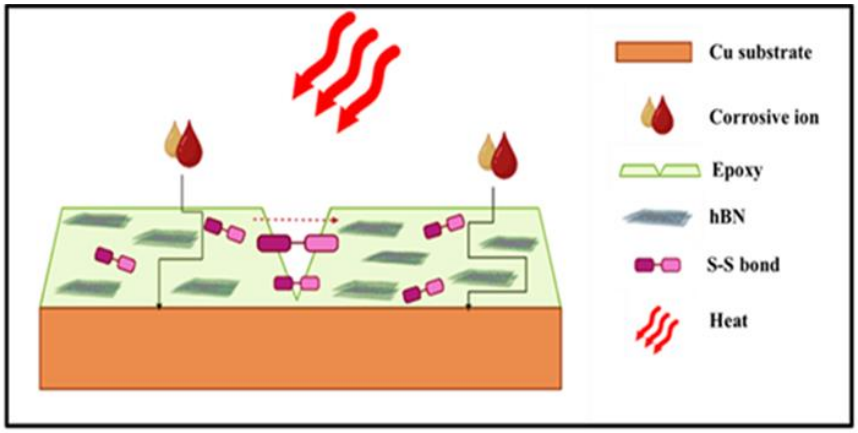

Figure 7. Schematic illustration of self-repair and corrosion protection mechanism.

Mechanism of Self-repairing and Corrosion Protection

Figure 7 suggests the overall mechanism of self-repairable and corrosion protection of EV-*x*hBN nanocomposite coating. The prepared nanocomposite coating could repair the damaged area through heat exposure. It also protected the underlying matrix from corrosion caused by the corrosive medium. The self-repairing effect was achieved owing to disulfide-mediated radical exchanges and S–S bond rearrangement in the epoxy matrix. The incorporation of highly conductive hBN improved thermal management in the epoxy matrix, increasing the ability of the disulfide bond exchange reaction, hence, showing better self-repairing effect [28]. In addition, the presence of hBN creates a "labyrinth effect" that lengthens the penetration path of corrosive ions to the substrate, thus increasing the corrosion resistance of the coating [29].

CONCLUSION

The mechanical integrity, wettability, self-repairable characteristics, and corrosion resistance performance of EV, and EV-*x*hBN nanocomposite coatings were successfully investigated. The EV-0.5hBN coating rapidly self-repaired at 10 minutes time denoting lower dose of hBN adequately provide superior performance. Meanwhile, higher loading positively impacts the corrosion resistance behaviour of Cu and reduce the corrosion rate (~0.004 mm/yr). The EV-1hBN coating also showed higher water contact angle which is beneficial for anti-corrosion performance. These results demonstrate that self-repair performance is optimized at low hBN loadings, whereas corrosion resistance is enhanced at higher loadings. Such insights are crucial for designing advanced protective coatings for industrial applications.

ACKNOWLEDGEMENTS

The authors would like to acknowledge the funding from the Ministry of Education Malaysia in the form of [RDU243708: FRGS-EC/1/2024/STG05/UMPSA/02/1] and Universiti Malaysia Pahang Al-Sultan Abdullah in the form of grant RDU240335 and technical staff for the research support.

REFERENCES

1. Peng, Bokai, Zongxue Yu, Haidong Chen, Kexi Liao, Yuchi Guo, Junlei Tang and Haojue Wen (2023) Boron Nitride and ZIF-67 Composite Material to Improve the Long Term Corrosion Resistance of Epoxy Resin Coating. *Diamond and Related Materials*, **139**, 110299.

2. Ye, Yuwei, Hao Chen, Yangjun Zou, Ying Ye and Haichao Zhao (2020) Corrosion Protective Mechanism of Smart Graphene-Based Self-Healing Coating on Carbon Steel. *Corrosion Science*, **174**, 108825.

3. Attaei, Mahboobeh, Lénia M. Calado, Maryna G. Taryba, Yegor Morozov, R. Abdul Shakoor, Ramazan Kahraman, Ana C. Marques and M. Fátima Montemor (2020) Autonomous Self-Healing in Epoxy Coatings Provided by High Efficiency Isophorone Diisocyanate (IPDI) Microcapsules for Protection of Carbon Steel. *Progress in Organic Coatings*, **139**, 105445.

4. Ahmad, S., Habib, S., Nawaz, M., Shakoor, R. A., Kahraman, R. & Al Tahtamouni, T. M. (2023) The role of polymeric matrices on the performance of smart self-healing coatings: A review. *Journal of Industrial and Engineering Chemistry*, **124**, 40–67.

5. Singh, P., Rao, A. U., Sharma, H., Bohra, B. S., Dagar, T., Sahoo, N. G. & Patel, R. (2024) Microwave assisted self-repairable vitrimeric coating for anti-corrosive applications. *Progress in Organic Coatings*, **191**, 108411.

6. Sanka, R. S. P., Rana, S., Singh, P., Mishra, A. K., Kumar, P., Singh, M. & Park, C. (2023) Self-healing nanocomposites via N-doped GO promoted "click chemistry". *Soft Matter*, **19(1)**, 98–105.

7. Chang, Y., Yan, X. & Wu, Z. (2023) Application and prospect of self-healing microcapsules in surface coating of wood. *Colloid and Interface Science Communications*, **56**, 100736.

8. Zhang, F., Ju, P., Pan, M., Zhang, D., Huang, Y., Li, G. & Li, X. (2018) Self-healing mechanisms in smart protective coatings: A review. In *Corrosion Science*, **144**, 74–88.

9. Krishnakumar, B., Sanka, R. S. P., Binder, W. H., Park, C., Jung, J., Parthasarthy, V. & Yun, G. J. (2020) Catalyst free self-healable vitrimer/ graphene oxide nanocomposites. *Composites Part B: Engineering*, **184**, 107647.

10. de Luzuriaga, A. R., Martin, R., Markaide, N., Rekondo, A., Cabañero, G., Rodríguez, J. & Odriozola, I. (2016) Epoxy resin with exchangeable disulfide crosslinks to obtain reprocessable, repairable and recyclable fiber-reinforced thermoset composites. *Materials Horizons*, **3(3)**, 241–247.

11. Krishnakumar, B., Sanka, R. P., Binder, W. H., Parthasarthy, V., Rana, S. & Karak, N. (2020) Vitrimers: Associative dynamic covalent adaptive networks in thermoset polymers. *Chemical Engineering Journal*, **385**, 123820.

12. Zhang, B., Fan, H., Xu, W. & Duan, J. (2022) Thermally triggered self-healing epoxy coating towards sustained anticorrosion. *Journal of Materials Research and Technology*, **17**, 2684–2689.

13. Yu, R. & Yuan, X. (2024) Rising of boron nitride: A review on boron nitride nanosheets enhanced anti-corrosion coatings. *Progress in Organic Coatings*, **186**, 107990.

14. Arenal, R. & Lopez-Bezanilla, A. (2015) Boron nitride materials: an overview from 0D to 3D (nano) structures. *Wiley Interdisciplinary Reviews: Computational Molecular Science*, **5(4)**, 299–309.

15. Mazhar, H., Adamson, D. H. & Al-Harthi, M. A. (2023) Differently oxidized portions of functionalized hexagonal boron nitride. *Materials Chemistry and Physics*, **308**, 128243.

16. Prasai, D., Tuberquia, J. C., Harl, R. R., Jennings, G. K. & Bolotin, K. I. (2012) Graphene: corrosion-inhibiting coating. *ACS Nano*, **6(2)**, 1102–1108.

17. Zhang, B., Fan, H., Xu, W. & Duan, J. (2022) Thermally triggered self-healing epoxy coating towards sustained anti-corrosion. *Journal of Materials Research and Technology*, **17**, 2684–2689.

18. Küçükdoğru, R., Türkez, H., Arslan, M. E., Tozlu, Ö. Ö., Sönmez, E., Mardinoğlu, A. & Di Stefano, A. (2020) Neuroprotective effects of boron nitride nanoparticles in the experimental Parkinson's disease model against MPP+ induced apoptosis. *Metabolic Brain Disease*, **35(6)**, 947–957.

19. Usman, U. L., Allam, B. K., Singh, N. B. & Banerjee, S. (2022) Adsorptive removal of Cr (VI) from wastewater by hexagonal boron nitride-magnetite nanocomposites: Kinetics, mechanism and LCA analysis. *Journal of Molecular Liquids*, **354**, 118833.

20. Chen, H., Yu, Z., Yang, G., Liao, K., Peng, B., Guo, Y. & Zhu, L. (2022) A hydrophobic smart coating based on hexagonal boron nitride/ metal-organic frameworks for high-performance corrosion protection. *Progress in Organic Coatings*, **172**, 107154.

21. Chau, T. T., Bruckard, W. J., Koh, P. T. L. & Nguyen, A. V. (2009) A review of factors that affect contact angle and implications for flotation practice. *Advances in Colloid and Interface Science*, **150(2)**, 106–115.

22. Zhang, B., Fan, H., Xu, W. & Duan, J. (2022) Thermally triggered self-healing epoxy coating towards sustained anti-corrosion. *Journal of Materials Research and Technology*, **17**, 2684–2689.

23. Cao, Y., Wang, X., Wu, J., Xu, Y., Gerard, J. F., Jiang, L. & Dai, L. (2022) A novel self-healing and removable hexagonal boron nitride/epoxy coating with excellent anti-corrosive property based on Diels-Alder reaction. *Progress in Organic Coatings*, **173**, 107209.

24. Joy, J., George, E., Thomas, S. & Anas, S. (2020) Effect of filler loading on polymer chain confinement and thermomechanical properties of epoxy/boron nitride (h-BN) nanocomposites. *New Journal of Chemistry*, **44(11)**, 4494–4503.

25. Gao, X., Bilal, M., Ali, N., Yun, S., Wang, J., Ni, L. & Cai, P. (2020) Two-dimensional nanosheets functionalized water-borne polyurethane nano-

composites with improved mechanical and anti-corrosion properties. *Inorganic and Nano-Metal Chemistry*, **50(12)**, 1358–1366.

26. Verma, C., Dubey, S., Barsoum, I., Alfantazi, A., Ebenso, E. E. & Quraishi, M. A. (2023) Hexagonal boron nitride as a cutting-edge 2D material for additive application in anticorrosive coatings: Recent progress, challenges and opportunities. *Materials Today Communications*, **35**, 106367.

27. Lorwanishpaisarn, N., Srikhao, N., Jetsrisuparb, K., Knijnenburg, J. T., Theerakulpisut, S., Okhawilai, M. & Kasemsiri, P. (2022) Self-healing ability of epoxy vitrimer nanocomposites containing bio-based curing agents and carbon nanotubes for corrosion protection. *Journal of Polymers and the Environment*, **30(2)**, 472–482.

28. Liu, J., Feng, H., Dai, J., Yang, K., Chen, G., Wang, S. & Liu, X. (2023) A Full-component recyclable Epoxy/BN thermal interface material with anisotropy high thermal conductivity and interface adaptability. *Chemical Engineering Journal*, **469**, 143963.

29. Wan, S., Chen, H., Liao, B. & Guo, X. (2024) Enhanced anti-corrosive capability of waterborne epoxy coating by ATT exfoliated boron nitride nanosheets composite fillers. *Progress in Organic Coatings*, **186**, 108089.